Modeling of temperatures by using the algorithm of queue burning movement in the UCG Process

Milan Durdán [1] *and* ***Karol Kostúr*** [2]

In this contribution, a proposal of the system for indirect measurement temperatures in the underground coal gasification (UCG) process is presented. A two-dimensional solution results from the Fourier partial differential equation of the heat conduction was used for the calculation of the temperature field in the real coal seam. An algorithm of queue burning movement for modeling the boundary conditions in gasification channel was created. Indirect measurement temperatures system was verified in the laboratory conditions.

Key words: *UCG, indirect measurement, physical model, algorithm, simulation model.*

Introduction

Underground coal gasification (UCG) is an industrial process that provides an alternative to conventional underground mining at coal seams that are located especially deep underground. This process converts coal into product gas (syngas). The product gas composition depends on coal geology and gasification parameters. It is necessary to build a system of two wells (inlet and outlet) which are drilled from Earth's surface to the coal seam. These two wells are interlinked by a channel that is drilled through the coal seam before the start of UCG process. The coal seam is ignited, and gas mixture is injected into the inlet well, after linked inlet and outlet well. The inlet gas mixture (oxidizing mixture) consists of a ratio of components: air, O_2, H_2O and CO_2. The control of the ratio of these components stabilizes coal seam temperature on the desired value. This temperature allows the start of chemical reactions, which are needed to create syngas with higher calorific value. The whole UCG reactor can be divided into three zones: oxidation zone, reducing zone and drying and pyrolysis zone. The reactions that take place in these zones depend on coal geology, oxidizer composition, and temperature height. The oxidation reactions that increase the coal seam temperature (above 900°C) take place in the oxidation zone. The gasification reactions that generate the desired syngas (a mixture consists of CO, CH_4, and H_2) take place in the reduction zone. The temperatures range from 550 to 900°C in this zone. The coal seam is initially dried and then pyrolyzed in drying and pyrolysis zone, which takes place at temperatures ranging from 200 to 550°C. The product gas is cleaned and stored after its extracting from outlet well [1] [2] [3]. Scheme of the UCG process is shown in Fig.1.

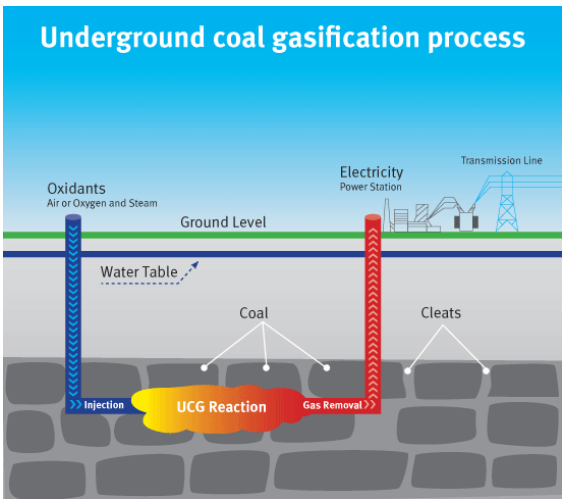

Fig. 1. Underground coal gasification process [4].

[1] *Ing. Milan Durdán, PhD.*, TU of Košice, F. BERG, Institute of Control and Informatization of Production Processes, B.Němcovej 3, Košice, Slovak Republic milan.durdan@tuke.sk.

[2] *Prof. Ing. Karol Kostúr, CSc.*, TU of Košice, F. BERG, Institute of Control and Informatization of Production Processes, B.Němcovej 3, Košice, Slovak Republic karol.kostur@tuke.sk .

The temperature range is characteristic for individual zones. It follows that the temperature control is needed in the UCG reactor for the setting of these zones. The existence of information about controlled variable is a necessary condition for the process control, but the temperature in UCG reactor is not possible to measure. The cause is, for example, an aggressive environment and the impossibility of thermocouples location in the whole real coal seam. The indirect measurement of temperature is one possible solution to this problem. The paper describes the design of the indirect measurement temperatures system in the UCG reactor based on a mathematical model in the form of the simulation model. The simulation model is supplemented by algorithm queue burning movement for modeling the boundary conditions in gasification channel. The coal seam temperatures are calculated based on measured temperatures in the surrounding rocks and atmospheric temperature above the earth's surface.

The system for indirect measurement temperatures is created by adjusting the model described in the article [5]. This model calculates coal seam temperatures based on measured temperatures of surrounding rocks, earth surface temperatures and heat of the inner source. It was verified by an experiment realized in the physical model of the gasifier (Generator) that simulates the conditions of the real coal-bed in geometric similarity. The simulation of the UCG process in the created generator (Fig. 2) is based on the principle of regulated supply of the oxidizer (input of the oxidizer) into the burning coal seam and exhaust of the produced syngas (output of the gas). Sounds for the local extraction and analysis of the syngas are placed on the lid of the generator. Coal seam model embedded into generator consists of the overburden, underbed and coal. It is arranged so that the air is able to permeate through the whole coal seam [6] [7].

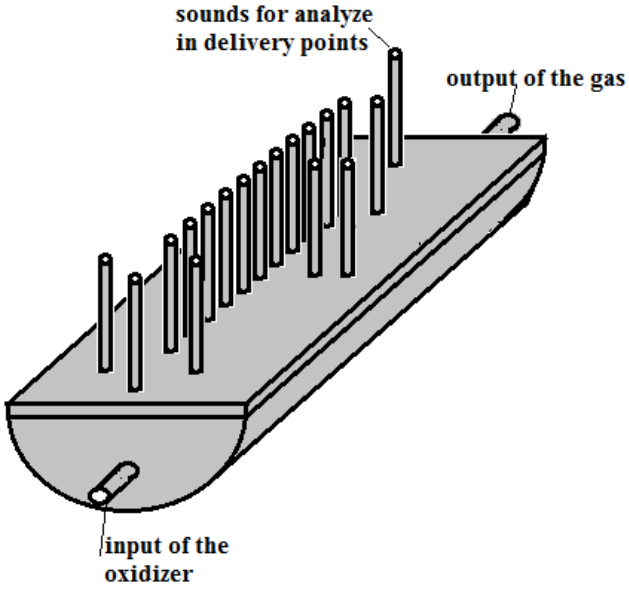

Fig. 2. Gasification generator.

In the design of a system of indirect measurement temperatures, the authors also arose from previous knowledge of solution of indirect measurement temperatures in the annealing process of steel coils. The indirect measurement models were based on elementary balances method adjusted first for a one-dimensional temperature field solution and in second variants for a two-dimensional temperature field solution. The authors in [8] created an indirect measurement system based on the elementary balance method adjusted for the solution of one-dimensional temperature field with boundary conditions of the first type. The temperature in the annealed coil was calculated based on its surface temperature measured on the outer and inner surface. The indirect measurement system was supplemented by heat conductivity adaptation and verified on the laboratory measurements. The resulting accuracy of the model in the form of relative error was in the range from 3.3 to 5.95 %. Authors in [9] adjusted the elementary balances method for solving a two-dimensional temperature field and supplemented the method in the form of differential equations for the calculation of steel coil surface temperature based on directly measured atmosphere temperature. Relative error was in the range from 4.3 to 6.1 % at operating measurements. The indirect measurement system has been extended to the surface temperature calculation with the use of neural networks in Article [10]. The accuracy was determined by calculating the relative error for the operating measurement and its value ranged from 4.8 to 7.3%. Authors in [11] verified that system of indirect measurement of heat flows falling on the thermally treated charge that was steel coil. Indirectly measured heat flows were entering to the elementary balances method expressed for the boundary conditions of the second type. The relative error at inner temperatures was fluctuating between 3.52 to 21.39 %.

Mathematical model of the UCG process

The system of indirect measurement temperatures for the solution of the temperature field in the real coal seam (respectively generator) is based on a mathematical model in the form of a two-dimensional solution of the Fourier partial differential equation of the heat conduction in the following form [12], [13], [14]:

$$\frac{\partial(\rho,c,T)}{\partial\tau}=\frac{\partial\left(\lambda\frac{\partial T}{\partial x}\right)}{\partial x}+\frac{\partial\left(\lambda\frac{\partial T}{\partial y}\right)}{\partial y} \tag{1}$$

where c is the specific heat capacity of the material (J.kg^{-1}.K^{-1}), ρ is the material density (kg.m^{-3}), λ is material heat conductivity (W.m^{-1}.K^{-1}), T is temperature (K), τ is time (s), x, y are coordinates of the point in space (m).

The elementary balances method [15], [16], [17] was used for the solution of Fourier partial differential equation. The elementary balance method results from dividing of the real seam or physical model to the elementary cuboids. For all elementary cuboids, the balance equation was formulated, and the implicit algorithm of temperature field solution was used. In Fig. 3, the scheme of dividing the part of the real seam (respectively generator) on elementary cuboids is shown, where the mass and temperature are centered at their centroids.

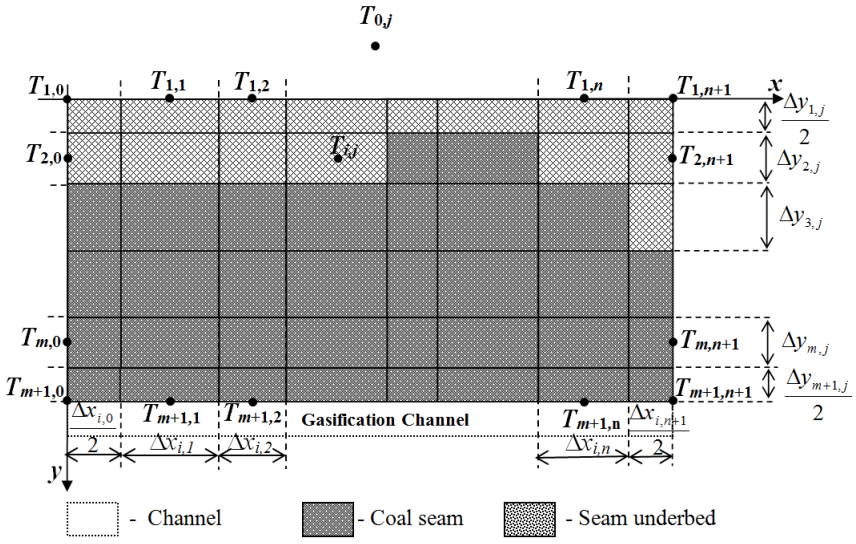

Fig. 3. The dividing of the coal seam to the elementary cuboids.

From the Fig. 3 results following:

- $\Delta x_{i,0}, \Delta x_{i,1}, \Delta x_{i,2}, \ldots, \Delta x_{i,j}, \ldots, \Delta x_{i,n+1}$ is dimension of the elementary cuboid in the direction of the x-axis where i = 1, 2, ..., m+1,
- $\Delta y_{1,j}, \Delta y_{2,j}, \Delta y_{3,j}, \ldots, \Delta y_{i,j}, \ldots, \Delta y_{m+1,j}$ is dimension of the elementary cuboid in the direction of the y-axis where j = 0, 1, ..., n+1,
- $T_{i,j}$ is temperature in the node point i, j where i=1, 2, …, m+1 and j=0, 1, …, n+1,
- $T_{0,j}$ is atmosphere temperature where j=0, 1, …, n+1.

The inner elementary cuboid volume, corner elementary cuboid volume and surface elementary cuboid volume in the considered two-dimensional objects was formulated in [5].

The created mathematical model includes the heat transfer by conduction in the direction of the axis x and y in the coal seam and heat transfer by convection in the direction of the axis y between atmosphere temperature and the top surface temperature of the overburden (the earth surface temperature at the real seam or top surface temperature of the generator).

The solution of the Fourier partial differential equation of the heat conduction is based on the border conditions that are divided on initial and boundary conditions:

The initial condition is a known arrangement of the temperature field ($T_{i,j}$ for a pair of coordinates i=0, 1, …, m+1 and j=0, 1, …, n+1) at the time zero $\tau = 0$.

Boundary conditions for a defined part of the real seam (from gasification channel to the upper surface) are considered in the following three forms:

1. Surrounding rocks temperature of coal seam as a time function:

a) $T_{i,0}$ for coordinate i=1, 2, …, m,
b) $T_{i,n+1}$ for coordinate i=1, 2, …, m,

2. Coal surface temperature in gasification channel as a time function: $T_{m+1,j}$ for coordinate j=0, 1, …, n+1.
3. Atmosphere temperature as a time function: $T_{0,j}$ for coordinate j=0, 1, …, n+1.

The total number of elementary cuboids with unknown temperature $T_{i,j}$ in the node point i, j is equal to m x n where i=1, 2, …, m and j=1, 2, …, n.

The following balance equations apply for the node point on the coordinates i, j.

For pair of coordinates i=2, 3, …, m and j=1, 2, …, n applies:

$$\left[\left(q^{y}_{i-1,j}-q^{y}_{i,j}\right)\Delta x_{i,j}+\left(q^{x}_{i,j-1}-q^{x}_{i,j}\right)\Delta y_{i,j}\right]\Delta\tau = \\ =\Delta x_{ij}\cdot\Delta y_{ij}\cdot\left(\rho_{i,j}(\tau+\Delta\tau)\cdot c_{i,j}(\tau+\Delta\tau)\cdot T_{i,j}(\tau+\Delta\tau)-\rho_{i,j}(\tau)\cdot c_{i,j}(\tau)\cdot T_{i,j}(\tau)\right) \tag{2}$$

For pair of coordinates i=1 and j=1, 2, …, n applies:

$$\left[\left(q^{y,con}_{i-1,j}-q^{y}_{i,j}\right)\Delta x_{i,j}+\left(q^{x}_{i,j-1}-q^{x}_{i,j}\right)\frac{\Delta y_{i,j}}{2}\right]\Delta\tau = \\ =\Delta x_{ij}\cdot\frac{\Delta y_{ij}}{2}\cdot\left(\rho_{i,j}(\tau+\Delta\tau)\cdot c_{i,j}(\tau+\Delta\tau)\cdot T_{i,j}(\tau+\Delta\tau)-\rho_{i,j}(\tau)\cdot c_{i,j}(\tau)\cdot T_{i,j}(\tau)\right) \tag{3}$$

Heat flow density is calculated according to the following relations:

$$q^{y}_{i-1,j}=\frac{\lambda_{i-1,j;i,j}}{\frac{\Delta y_{i-1,j}}{2}+\frac{\Delta y_{i,j}}{2}}\cdot\left(T_{i-1,j}-T_{i,j}\right) \tag{4}$$

$$q^{y}_{i,j}=\frac{\lambda_{i,j;i+1,j}}{\frac{\Delta y_{i,j}}{2}+\frac{\Delta y_{i+1,j}}{2}}\cdot\left(T_{i,j}-T_{i+1,j}\right) \tag{5}$$

$$q^{x}_{i,j-1}=\frac{\lambda_{i,j-1;i,j}}{\frac{\Delta x_{i,j-1}}{2}+\frac{\Delta x_{i,j}}{2}}\cdot\left(T_{i,j-1}-T_{i,j}\right) \tag{6}$$

$$q^{x}_{i,j}=\frac{\lambda_{i,j;i,j+1}}{\frac{\Delta x_{i,j}}{2}+\frac{\Delta x_{i,j+1}}{2}}\cdot\left(T_{i,j}-T_{i,j+1}\right) \tag{7}$$

$$q^{y,con}_{i-1,j}=\alpha\cdot\left(T_{i-1,j}-T_{i,j}\right) \tag{8}$$

where $q^{y}_{i-1,j}$ is heat flow density by condition between elementary cuboids with temperature $T_{i-1,j}$ and $T_{i,j}$ (W.m^{-2}), $q^{y}_{i,j}$ is heat flow density by condition between elementary cuboids with temperature $T_{i,j}$ and $T_{i+1,j}$ (W.m^{-2}), $q^{x}_{i,j-1}$ is heat flow density by condition between elementary cuboids with temperature $T_{i,j-1}$ and $T_{i,j}$ (W.m^{-2}), $q^{x}_{i,j}$ is heat flow density by condition between elementary cuboids with temperature $T_{i,j}$ and $T_{i,j+1}$ (W.m^{-2}), $q^{y,con}_{i-1,j}$ is heat flow density by convection between elementary cuboids with temperature $T_{0,j}$ and $T_{1,j}$ (W.m^{-2}), α is heat transfer coefficient by convection (W.m^{-2}.K^{-1}), $\lambda_{i-1,j;i,j}$ is heat conductivity between elementary cuboids with temperature $T_{i-1,j}$ and $T_{i,j}$ (W.m^{-1}.K^{-1}), $\lambda_{i,j;i+1,j}$ is heat conductivity between elementary cuboids with temperature $T_{i,j}$ and $T_{i+1,j}$ (W.m^{-1}.K^{-1}), $\lambda_{i,j-1;i,j}$ is heat conductivity between elementary cuboids with temperature $T_{i,j-1}$ and $T_{i,j}$ (W.m^{-1}.K^{-1}), $\lambda_{i,j;i,j+1}$ is heat conductivity between elementary cuboids with temperature $T_{i,j}$ and $T_{i,j+1}$ (W.m^{-1}.K^{-1}), $c_{i,j}$ is specific heat capacity of the material in i, j elementary cuboid (J.kg^{-1}.K^{-1}), $\rho_{i,j}$ is material density in i, j elementary cuboid (kg.m^{-3}), $\Delta x_{i,j}$ is dimension of the elementary cuboid in direction of the x axis (m), $\Delta y_{i,j}$ is dimension of the elementary cuboid in the direction of the y axis (m), $\Delta\tau$ is time step (s), $V_{i,j}$ is elementary cuboid volume in the node point i, j (m^3), $T_{i,j}$ is temperature in the node point i, j (K).

Thermophysical properties (λ, ρ and c) used in the mathematical model depend on the type of rock and the temperature of the elementary cuboid.

Time step of calculation $\Delta\tau$ is estimated from term of stability:

$$\Delta\tau \leq \min \frac{c_{i,j} \cdot \rho_{i,j}}{2 \cdot \lambda_{i,j} \cdot \left(\frac{1}{\Delta x_{i,j}^2} + \frac{1}{\Delta y_{i,j}^2} \right)} \tag{9}$$

After the substitution of heat flow densities represented by equations (4) to (8) into the system of equations represented by equations (2) and (3), we get $m \times n$ linear equations (10) with unknown $T_{i,j}$ (i=1,2, ..., m; j =1,2, ..., n). Subsequently, a new thermal field in time $\tau + \Delta\tau$ is obtained by the calculation of this system of linear equations.

$$\begin{aligned}
&a_{11}T_{11} + a_{12}T_{12} + \quad + a_{1,n+1}T_{21} && = b_1 \\
&a_{21}T_{11} + a_{22}T_{12} + a_{23}T_{13} + \quad + a_{2,n+2}T_{22} && = b_2 \\
&\vdots \\
&\quad a_{n,(n-1)}T_{1(n-1)} + a_{n,n}T_{1n} + \quad + a_{n,n\cdot 2}T_{2n} && = b_n \\
&\vdots \\
&a_{n+1,1}T_{11} + \quad + a_{n+1,(n+1)}T_{21} + a_{n+1,(n+2)}T_{22} + \quad + a_{n+1,(n\cdot 2+1)}T_{31} && = b_{n+1} \\
&\quad a_{n+2,2}T_{12} + \quad + a_{n+2,(n+1)}T_{21} + a_{n+2,(n+2)}T_{22} + a_{n+2,(n+3)}T_{23} + + a_{n+2,(n\cdot 2+2)}T_{32} && = b_{n+2} \\
&\vdots \\
&\quad a_{n\cdot 2,n}T_{1n} + \quad + a_{n\cdot 2,(n+(n-1))}T_{2(n-1)} + a_{n\cdot 2,(n\cdot 2)}T_{2n} + \quad + a_{n\cdot 2,n\cdot 3}T_{3n} && = b_{n\cdot 2} \\
&\vdots \\
&a_{(n\cdot m)-(n-1),(n\cdot m)-(n+n-1)}T_{(m-1)1} + \quad + a_{(n\cdot m)-(n-1),(n\cdot m)-(n-1)}T_{m1} + a_{(n\cdot m)-(n-1),(n\cdot m)-(n-2)}T_{m2} && = b_{(n\cdot m)-(n-1)} \\
&a_{(n\cdot m)-(n-2),(n\cdot m)-(n+n-2)}T_{(m-1)2} + \quad + a_{(n\cdot m)-(n-2),(n\cdot m)-(n-1)}T_{m1} + a_{(n\cdot m)-(n-2),(n\cdot m)-(n-2)}T_{m2} + \quad + a_{(n\cdot m)-(n-2),(n\cdot m)-(n-3)}T_{m3} && = b_{(n\cdot m)-(n-2)} \\
&\vdots \\
&\quad a_{(n\cdot m),(n\cdot m)-n}T_{(m-1)n} + \quad + a_{(n\cdot m),(n\cdot m)-1}T_{m(n-1)} + a_{(n\cdot m),(n\cdot m)}T_{mn} && = b_{(n\cdot m)}
\end{aligned} \tag{10}$$

Simulation model of the UCG process

A simulation model of the UCG process for modeling of the temperatures in the real seam was created. The simulation model is based on the described mathematical model. It can emulate the processes of UCG that run on the physical model (generator) or in the real seam. The scheme is shown in Fig. 4.

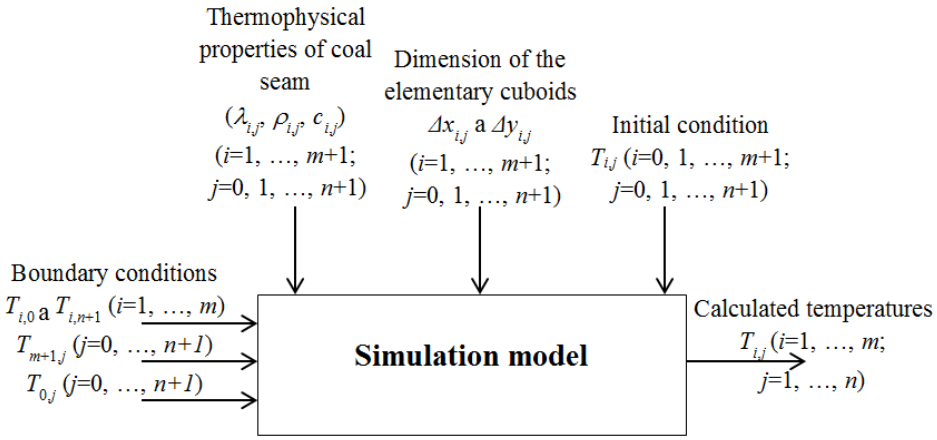

Fig. 4. Scheme of the simulation model.

The simulation model can calculate the temperature in node points of the temperature field based on initial temperatures (initial condition), temperatures from previous time step (boundary condition), thermophysical properties of the coal seam and the dimension of the elementary cuboids. Thanks to this utility we can evaluate

the present limitations in UCG process and to propose some arrangements, i.e. in advance verified of proposed arrangements on the simulation model. The simulated model was created in C code, and PETSc method was used for the solution of system equations (10) because of the size of the real seam. The dividing of the real seam to the elementary cuboids of acceptable dimension forms a large system of equations. The solution of this system of equations is lengthy by usual methods.

PETSc method is used for the numerical solution of partial differential equations and related problems on high-performance computers. The Portable, Extensible Toolkit for Scientific Computation (PETSc) is a suite of data structures and routines that provide the building blocks for the implementation of large-scale application codes on parallel (and serial) computers. PETSc uses the MPI standard for all message-passing communication. PETSc includes an expanding suite of parallel linear, nonlinear equation solvers and time integrators that may be used in application codes written in Fortran, C, C++, Python, and MATLAB (sequential). PETSc provides many of the mechanisms needed within parallel application codes, such as parallel matrix and vector assembly routines [18].

The simulation model was extended by the algorithm of queue burning movement for modeling boundary condition $T_{m+1,j}$ for coordinate j=0, 1, …, n+1. The algorithm is based on a database of the measured coal surface temperatures ($T_{m+1,k}$ for k = 1, 2, ..., p where k is measured temperature index, and p is measured temperatures count) in gasification channel obtained from UCG process realized on a similar coal seam (Fig. 5).

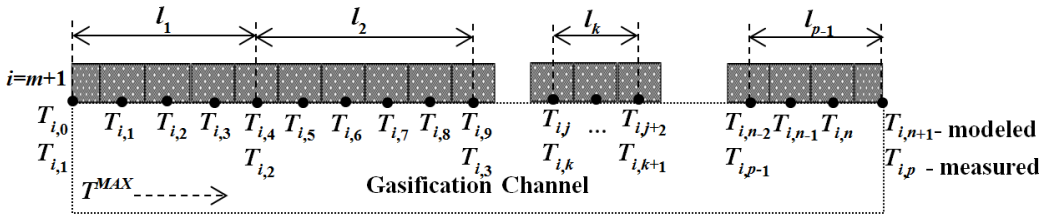

Fig. 5. Scheme of measured and modeled temperatures in gasification channel.

Measured temperatures are used for the calculation of the rate of thermal wave movement in gasification channel. It will ensure that the queue burning movement represents the movement of the temperature T^{MAX} ($T_{i,k+1}$) in gasification channel (index j) between temperatures $T_{i,k}$ and $T_{i,k+1}$.

The algorithm of queue burning movement can be divided into two main parts:

1. Calculation of the rate of thermal wave movement in gasification channel before the start of simulation process with using database temperatures ($T_{m+1,k}$ for k = 1, 2, ..., p) and distances (l_k for k = 1, 2, ..., p-1) between measured temperatures:
   a) Determination of maximal temperatures T_k^{MAX} and their times τ_k^{MAX} from behaviors of measured surface temperatures in gasification channel ($T_{m+1,k}$ for k = 1, 2, ..., p).
   b) Calculation of the rate of thermal wave movement between temperatures $T_{i,k}$ and $T_{i,k+1}$:

$$v_k = \frac{l_k}{\tau_{k+1}^{MAX} - \tau_k^{MAX}}$$

   where v_k is the rate of thermal wave movement for k = 1, 2, ..., p-1 (m.s^{-1}), l_k is the distance between temperatures with index k and k+1 (m), τ_k^{MAX} and τ_{k+1}^{MAX} are times of maximal temperatures with index k and k+1 obtained from behavior of measured temperatures $T_{i,k}$ and $T_{i,k+1}$ (s).
   Note:
   The resulting rate v_k between measuring points with index k and k+1 will be determined as an average rate from all rates if the database contains more temperature behaviors from one measurement point.

2. Determination of the amplitude coordinate (index j of the surface temperature $T_{m+1,j}$ in gasification channel) of the maximal temperature T^{MAX} ($T_{m+1,k+1}$) in process of simulation of UCG process if simulation time τ is from interval $\tau_k^{MAX} \le \tau < \tau_{k+1}^{MAX}$ (k = 1, 2, ..., p-1):
   a) Determination of distance of T^{MAX} from the k-th temperature ($T_{m+1,0}$) to the actual place of queue burning:

$$x^{MAX} = \sum_{i=1}^{k-1} l_i + \left(\tau - \tau_k^{MAX}\right) \cdot v_k$$

where τ is actual time of simulation, v_k is the rate of thermal wave movement between measuring points with index k and k+1.

b) Determination of maximal temperature index j^{MAX} of indexes j=0, 1, …, n+1 by minimization process:

$$\min_{d=0,1,\ldots,n} \left\{ \left| x^{MAX} - \sum_{j=0}^{d} \left(\frac{\Delta x_{m+1,j}}{2} + \frac{\Delta x_{m+1,j+1}}{2} \right) \right| \right\} \Rightarrow j^{MAX} = (d+1)$$

The algorithm adds the temperature T^{MAX} ($T_{m+1.\,j^{MAX}} = T^{MAX}$) to the group of measured temperatures. The number of known temperatures will increase about one at each time step. Boundary node points should correspond to points of measurement temperatures. The unknown temperature values are obtained, for example, by a linear approximation between the two measured temperatures if the number of node points is larger than the number of measured temperatures.

Results and discussion of simulation model verification

The inputs into simulation model were directly measured temperature of the atmosphere and channel temperatures on coal surface. Output was represented by an indirectly measured temperature in the coal seam. Measured temperatures were obtained from the experiment realized in the physical model (generator). The experiment was aimed at testing the uniflow system with non-separated coal. The model of the coal seam was created from 532 kg of coal. The layers were bedded as shown in Fig. 6. A channel along the entire length of the generator was created in the layer of under burden. Gasification channel was created by the following method: drilled coal blocks in the longitudinal direction were bound into the monolith and stored in the generator. The channel depth was 13 mm and width 10 mm. Three layers of coal were gradually bedded on the under burden. The thickness of coal seam was 340 mm. The sibral and nobasil are isolating materials for preclusion of the thermal loss to the environs. Individual overburden layers had these thicknesses: sibral – 30 mm, nobasil – 50 mm and sibral – 50 mm.

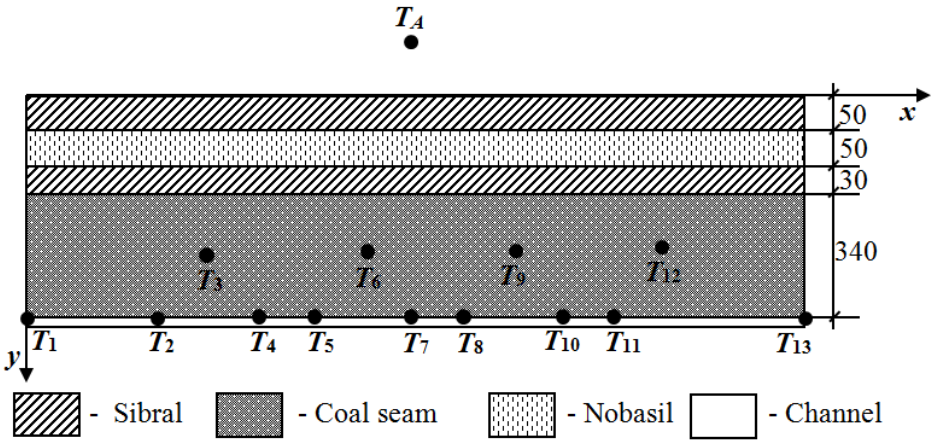

Fig. 6. Directly measured temperatures during the experiment.

Places of the temperature measurement by thermocouples in the Generator (temperatures in the gasification channel – T_1, T_2, T_4, T_5, T_7, T_8, T_{10}, T_{11}, T_{13}, temperatures in the coal seam – T_3, T_6, T_9, T_{12} and atmosphere temperatures T_A) during the experiment are schematically depicted in Fig. 6.

These measured temperatures were considered in the boundary conditions which are input to the simulation model:

1. Temperatures T_1, T_2, T_4, T_5, T_7, T_8, T_{10}, T_{11} and T_{13} for temperatures $T_{m+1,j}$ where j=0, 1, …, n+1.
2. Temperature T_A for temperatures $T_{0,j}$ where j=0, 1, …, n+1.

From the presented Fig. 6 results that temperatures along the height of the Generator were not measured ($T_{i,0}$ and $T_{i,n+1}$ for i = 1, 2 , ..., m). For this reason, the individual temperatures between the coal seam layers, sibral and nobasil, were determined by using the one-dimensional solution of the heat transfer in the direction

of the *y*-axis where the input from the bottom side are temperatures measured in the channel (T_1 as $T_{m+1,0}$ and T_{13} as $T_{m+1,n+1}$) and the atmosphere temperature is measured from the top side (T_A as $T_{0,0}$ and T_A as $T_{0,n+1}$).

For the one-dimensional heat conduction in the direction of the *y*-axis the Fourier equation of the heat conduction has the following form:

$$\frac{\partial(\rho, c, T)}{\partial \tau} = \frac{\partial\left(\lambda \frac{\partial T}{\partial y}\right)}{\partial y} \tag{11}$$

Also for the solution of one-dimensional heat conduction in the direction of the *y*-axis, the elementary balances method derived from the implicit algorithm of the temperature field solution was used. The following balance equations were applied to the node point on the coordinates *i*,*j*.

For pair of coordinates i=2, 3, …,m and j=0 and for pair coordinates i=2, 3, …,m and j=n+1 applies:

$$\left(q^{y}_{i-1,j} - q^{y}_{i,j}\right)\Delta\tau = \Delta y_{ij} \cdot \left(\rho_{i,j}(\tau+\Delta\tau)\cdot c_{i,j}(\tau+\Delta\tau)\cdot T_{i,j}(\tau+\Delta\tau) - \rho_{i,j}(\tau)\cdot c_{i,j}(\tau)\cdot T_{i,j}(\tau)\right) \tag{12}$$

For pair of coordinates i=1 and j=0 and for pair coordinates i=1 and j=n+1 applies:

$$\left(q^{y,con}_{i-1,j} - q^{y}_{i,j}\right)\Delta\tau = \frac{\Delta y_{ij}}{2} \cdot \left(\rho_{i,j}(\tau+\Delta\tau)\cdot c_{i,j}(\tau+\Delta\tau)\cdot T_{i,j}(\tau+\Delta\tau) - \rho_{i,j}(\tau)\cdot c_{i,j}(\tau)\cdot T_{i,j}(\tau)\right) \tag{13}$$

Heat flow density was calculated according to (4), (5) and (8) equations. Description of individual items of the equations is the same as in the section of the mathematical model.

After the substitution of the heat flow densities represented by equations (4), (5) and (8) into the system of equations represented by equations (12) and (13), we get m linear equations (14) with unknown $T_{i,0}$ (i=1,2, ..., m):

$$\begin{aligned}
a_{11}\cdot T_{1,0} + a_{12}\cdot T_{2,0} &= b_1 \\
a_{21}\cdot T_{1,0} + a_{22}\cdot T_{2,0} + a_{23}\cdot T_{3,0} &= b_2 \\
a_{32}\cdot T_{2,0} + a_{33}\cdot T_{3,0} + a_{34}\cdot T_{4,0} &= b_3 \\
&\vdots \\
a_{m-1,m-2}\cdot T_{m-2,0} + a_{m-1,m-1}\cdot T_{m-1,0} + a_{m-1,m}\cdot T_{m,0} &= b_{m-1} \\
a_{m,m-1}\cdot T_{m-1,0} + a_{mm}\cdot T_{m,0} &= b_m
\end{aligned} \tag{14}$$

and m linear equations (15) with unknown $T_{i,n+1}$ (i=1,2, ..., m).

$$\begin{aligned}
a_{11}\cdot T_{1,n+1} + a_{12}\cdot T_{2,n+1} &= b_1 \\
a_{21}\cdot T_{1,n+1} + a_{22}\cdot T_{2,n+1} + a_{23}\cdot T_{3,n+1} &= b_2 \\
a_{32}\cdot T_{2,n+1} + a_{33}\cdot T_{3,n+1} + a_{34}\cdot T_{4,n+1} &= b_3 \\
&\vdots \\
a_{m-1,m-2}\cdot T_{m-2,n+1} + a_{m-1,m-1}\cdot T_{m-1,n+1} + a_{m-1,m}\cdot T_{m,n+1} &= b_{m-1} \\
a_{m,m-1}\cdot T_{m-1,n+1} + a_{mm}\cdot T_{m,n+1} &= b_m
\end{aligned} \tag{15}$$

The boundary conditions are obtained by the calculation of system equations (14) for temperatures $T_{i,0}$ (i = 1, 2 , ..., m) and system equations (15) for temperatures $T_{i,n+1}$ (i = 1, 2 , ..., m).

A simulation with temperatures depicted in Fig. 7a (measured channel temperatures during the experiment) as boundary condition for $T_{m+1,j}$ (j=0,1, ..., n+1) was realized. The measured atmosphere temperature was used as boundary condition for $T_{0,j}$ (j=0,1, ..., n+1). The indirectly measured coal temperatures (simulated) were compared with the directly measured coal temperatures (measured) from the realized experiment (Fig. 7b) after the simulation.

The results of the simulations are depicted in Fig. 8. The comparison of directly measured temperature T_3 (T3-measured) and indirectly measured temperature T_3 (T3-simulated) is depicted in Fig. 8a. The comparison of directly measured temperature T_6 (T6-measured) and indirectly measured temperature T_6 (T6-simulated) is depicted in Fig. 8b. The comparison of directly measured temperature T_9 (T9-measured) and indirectly measured temperature T_9 (T9-simulated) is depicted in Fig. 8c. The comparison of directly measured temperature T_{12} (T12-measured) and indirectly measured temperature T_{12} (T12-simulated) is depicted in Fig. 8d. Fig. 8 indicates that indirectly measured temperature copies behavior of directly measured temperature, i.e. the mathematical model is fine in the qualitative aspect, but there are visible deviations between indirectly measured temperature and directly measured, i.e. the model is not sufficient in the quantitative aspect.

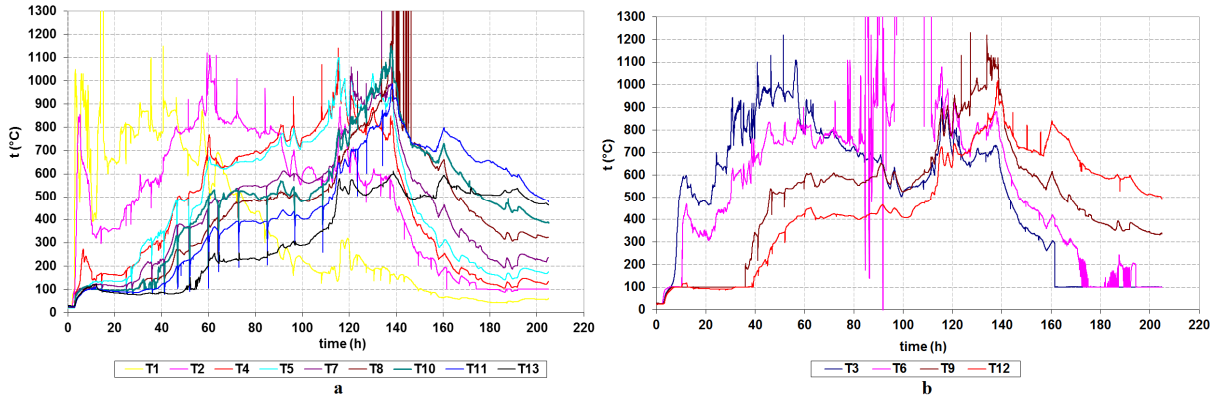

Fig. 7. Behaviors of the channel temperatures (a) and coal temperatures (b) [5].

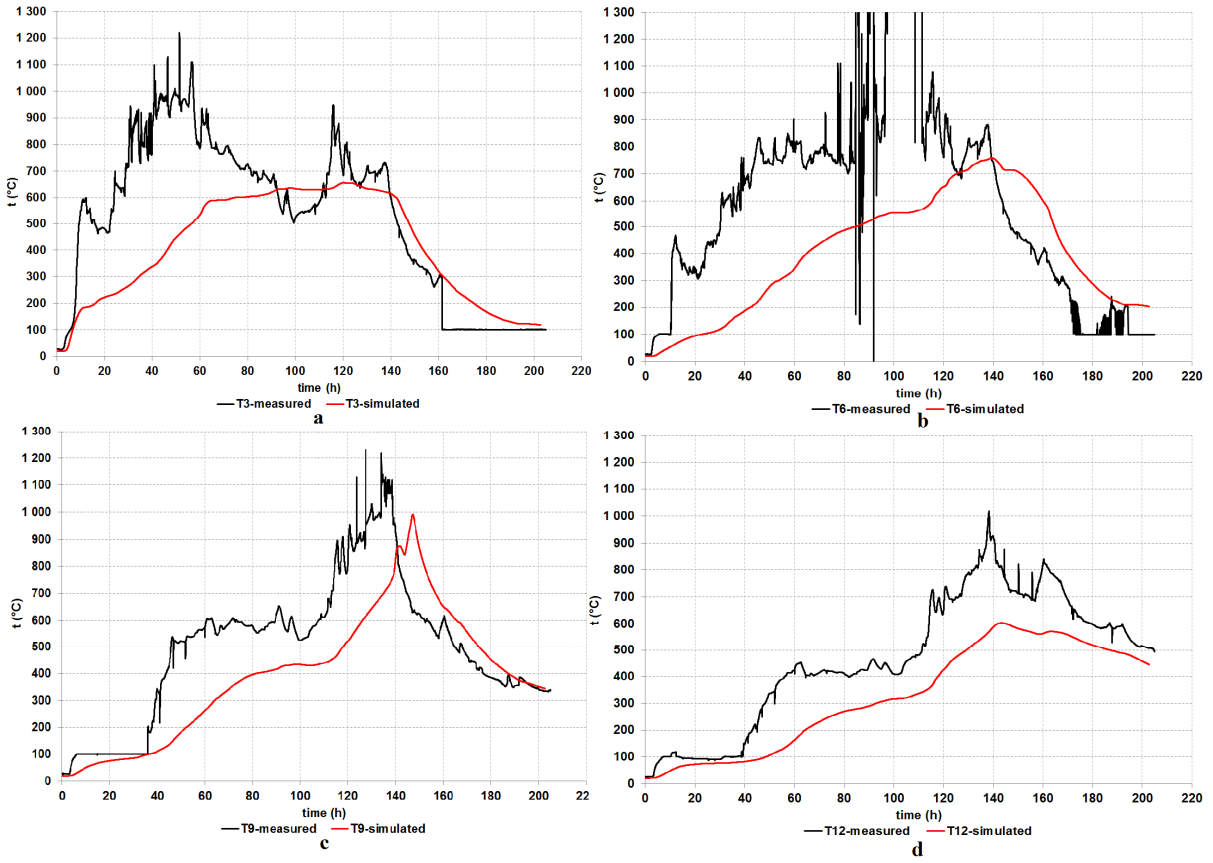

Fig. 8. Behaviors of the measured and simulated temperatures T3 (a), T6 (b), T9 (c), and T12 (d).

The model described in [5] was verified at the same channel and coal temperatures as the model described in this paper. The difference is that for boundary condition $T_{0,j}$ (j=0,1, ..., n+1), measured surface temperatures were used, the inner heat source was considered, and algorithm of queue burning movement was not considered. The average relative error described in [9] was used for the comparison of directly and indirectly measured temperatures for both models. It is shown in Tab. 1.

Tab. 1 indicates that the model described in this paper has a slightly lower accuracy (approximately 1 % at temperature T_3, T_9 and T_{12} and 5 % at temperature T_6) against the model described in [5]. The conformity between directly and indirectly measured temperatures was not improved, although variable boundary conditions were considered, and the algorithm of queue burning movement was used. It is also visible in Fig. 8.

Tab. 1. Relative error for individual temperatures.

Temperature [°C]	**Relative error** [%]	
	Model described in [5]	**Model described in this paper**
T3	40.95	41.90
T6	55.57	60.35
T9	31.02	32.04
T12	31.46	32.81

Conclusion

The numerical solutions of two-dimensional unsteady heat conduction equation for multi-layer overlying strata are obtained by an implicit form using the method of elementary balance, which meet the first kinds of boundary conditions. However, only one boundary condition is changeable, and it expresses the move of gasification front in gasification channel. Deviations between measured and simulated temperatures are probably caused by a fixed boundary condition in the direction of the axis "*y*" (Fig. 8). In other words, the move of gasification front has not been considered in this axis above UCG cavity. The reason for this fact is that the velocity of gasification front in the direction of the axis "*y*" was not evaluated during the UCG experiment. The extension of the mathematical model about these calculations can cause a decrease of deviations between directly and indirectly measured temperatures.

The information about behavior of the inner temperature in the coal seam enable to optimize the gasification process by a regulation of inputs (e.g. the ratio of the injected air, oxygen, H_2O and CO_2) and thereby to ensure the required growth of the temperature in the coal seam and behavior of the chemical reactions needed for the creation of the qualitative syngas. Implementation of this indirect measurement system to the practice can bring following:

- increase the quality of the syngas,
- save the money,
- the flexibility of solution perturbance in the UCG process.

Acknowledgment: *This work was partially supported by the project COGAR RFCR-CT-2013-00002, grant No. VEGA 1/0295/14 from the Slovak Grant Agency for Science and by grant No. APVV-14-0892.*

References

[1] Bhutto A. W., Bazmi A. A., Zahedi G.: Underground coal gasification: From fundamentals to applications. *Progress in Energy and Combustion Science 39 (2013) 189-214*.

[2] Uppal A. A., Bhatti A. I., Aamir E., Samar R., Khan S. A.: Control oriented modeling and optimization of one dimensional packed bed model of underground coal gasification. *Journal of Process Control 24 (2014) 269– 277.*

[3] Yang L.: Study on the model experiment and numerical simulation for underground coal gasification. *Fuel 3 (2004) 189–196.*

[4] Department of Environment and Heritage Protection: Underground coal gasification, *2013* [online] http://www.ehp.qld.gov.au/management/ucg/

[5] Durdán M., Kačur J.: Indirect temperatures measurement in UCG process. 14th International Carpathian Control Conference : May 26-29, 2013, *Rytro, Poland. - Piscataway : IEEE, 73-78.*

[6] Kačur J., Durdán M., Laciak M., Flegner P.: Impact analysis of the oxidant in the process of underground coal gasification. *Measurement 51 (2014) 147-155*.

[7] Laciak M., Škvareková E., Durdán, M., Kostúr K., Wittenberger G.: Study of underground coal gasification (UCG) technology in laboratory conditions. *Chem. Listy 106 (5) (2012) 384-391*.

[8] Durdán M., Kostúr K.: Adaptation of the system of indirect measurement of temperatures in the charge. Acta Montanistica Slovaca. *Vol. 11, no. 4 (2006), 264-272.*

[9] Laciak M., Durdán M., Kačur J.: Utilization of indirect measurement in the annealing process of the steel coils. *Acta Metallurgica Slovaca. Vol. 18, no. 1 (2012), 40-49.*

[10] Durdán M., Mojžišová A., Laciak M., Kačur J.: System for indirect temperature measurement in annealing process. *Measurement. Vol. 47, no. 1 (2014), 911-918.*

[11] Durdán M. , Kačur J.: System for Indirect Measurement of the Heat Flows at Annealing of the Steel Coils. *Acta Metallurgica Slovaca. Vol. 19, no. 2 (2013), 112-121*.

[12] Lin X., Zuotang W., Wengang H., Guojun K., Xuefeng L., Peng, Z. Jianhua W.: Temperature field distribution of burnt surrounding rock in UCG stope. *International Journal of Mining Science and Technology 24 (2014) 573-580.*

[13] Széplaky D., Varga A.: Mathematical model of temperature profile of the transit gas-pipeline laid in the ground. Annals of Faculty Engineering Hunedoara - *International Journal of Engineering. Vol. 12, no. 1 (2014) 223-226.*

[14] Széplaky D., Varga A., Kočanová S.: Analysis of the temperature field of the gas pipeline collector using cfd modeling. Annals of Faculty Engineering Hunedoara - *International Journal of Engineering. Vol. 12, no. 4 (2014) 123-130.*

[15] Kostúr K., et al.: Underground coal gasification by thermal decomposition no. APVV-0582-06, *Research Report of the Project, TU Košice, BERG, 2008*.

[16] Terpák J., Dorčák Ľ.. The processes of the heat transfer. *TU Košice, Faculty BERG, 2001*.

[17] Kostúr K.: Simulation models of the heat aggregates. *Publisher: Štroffek, Košice, 1997*.

[18] Balay S. et. al. Mathematics and Computer Science Division: PETSc Users Manual (Revision 3.5*), 2014*, http://www.mcs.anl.gov/petsc/petsc-current/docs/manual.pdf